

# We are IntechOpen, the world's leading publisher of Open Access books Built by scientists, for scientists

4,800

Open access books available

122,000

International authors and editors

135M

Downloads

Our authors are among the

154

Countries delivered to

TOP 1%

most cited scientists

12.2%

Contributors from top 500 universities



WEB OF SCIENCE™

Selection of our books indexed in the Book Citation Index  
in Web of Science™ Core Collection (BKCI)

Interested in publishing with us?  
Contact [book.department@intechopen.com](mailto:book.department@intechopen.com)

Numbers displayed above are based on latest data collected.  
For more information visit [www.intechopen.com](http://www.intechopen.com)



# Fully Automatic Technique for Liver Segmentation from Abdominal CT Scan with Knowledge-Based Constraints

Nader H. Abdel-massieh  
Menoufia University  
Egypt

## 1. Introduction

The proposed fully automatic technique and method to segment liver structure is divided into two sections: first section is *Pre processing steps and rough (initial) segmentation*; the second section is *refined segmentation (snake step)*, see Figure 1. The proposed automatic technique to detect tumor in liver parenchyma is also divided into two sections: first section

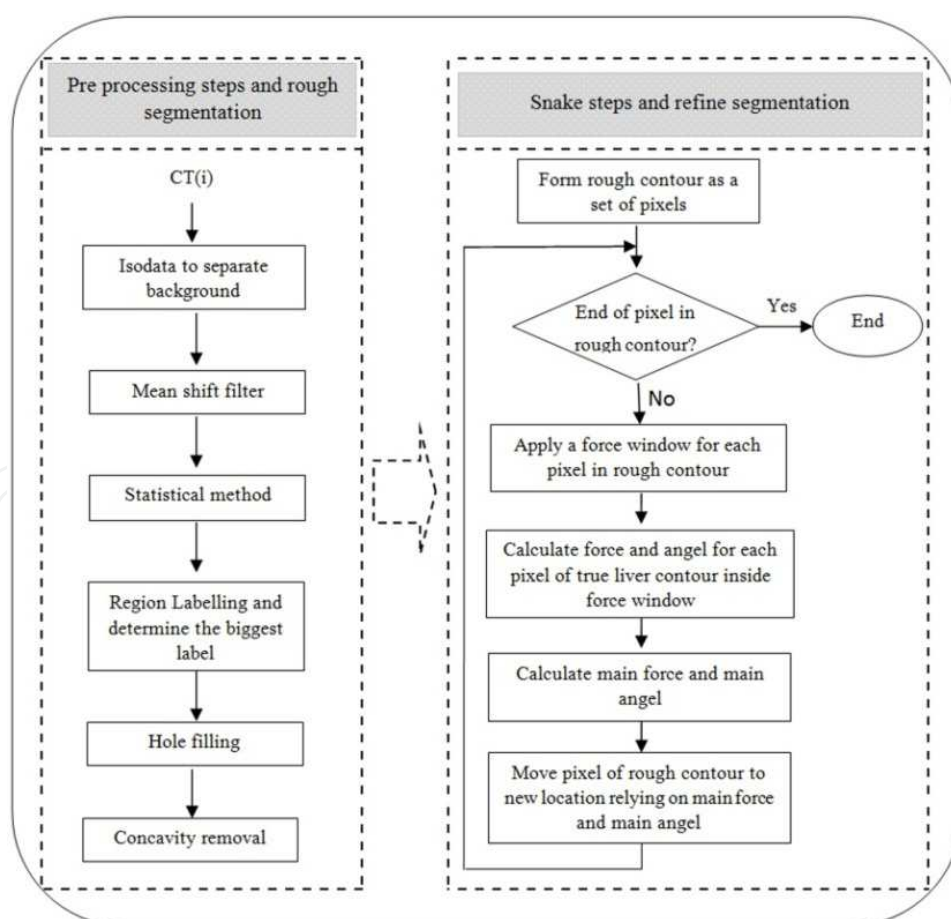


Fig. 1. Block diagram for the proposed fully automatic liver segmentation technique

*liver tumor segmentation* to detect any lesions; the second sections is *tumor classification* to differentiate between possible tumor and any other defect in CT slices, see Figure 2.

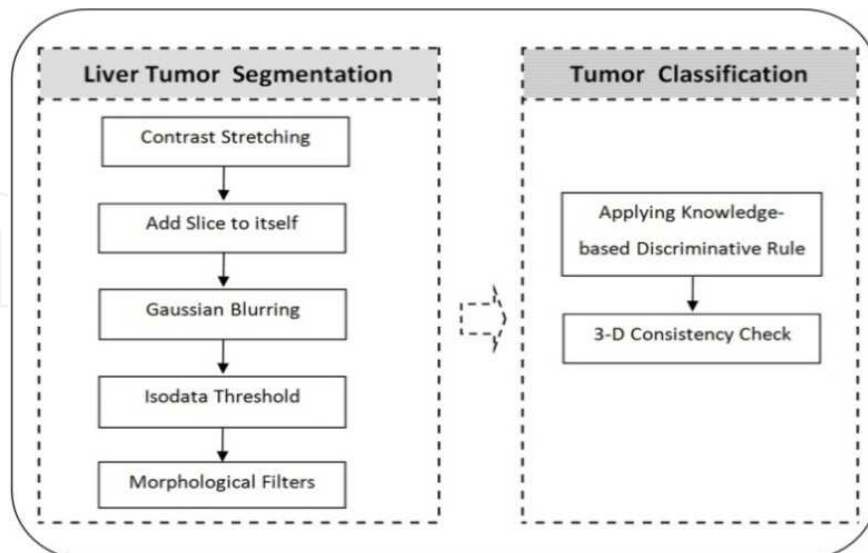


Fig. 2. Block diagram of the proposed automatic liver tumor detection technique

## 2. Liver segmentation

### 2.1 Preprocessing and rough segmentation

#### 2.1.1 Isodata

Before beginning the rough segmentation, the background of CT slice is separated using Isodata algorithm which it is one of the thresholding segmentation techniques. Isodata stands for Iterative Self-Organizing Data Analysis Techniques. The threshold is chosen from the brightness histogram of CT slice. The histogram is initially segmented into two parts using a starting threshold value such as  $\theta_0$  (where  $\theta$  is threshold value), half the maximum dynamic range. The sample mean ( $m_f, 0$ ) of the gray values associated with the foreground pixels and the sample mean ( $m_b, 0$ ) of the gray values associated with the background pixels are computed, see Figure 3. A new threshold value  $\theta_1$  is now computed as the average of these two sample means. The process is repeated, based upon the new threshold, until the threshold value does not change any more. In formula:

$$\theta_k = \frac{m_{f,k-1} + m_{b,k-1}}{2} \text{ until } \theta_k = \theta_{k-1} \quad (1)$$

After applying Isodata algorithm the outer area around patient's body will be eliminated, as seen in Figure 4, and this help in the reduction in computation time needed for following steps.

#### 2.1.2 Mean shift filter

In order to remove noise caused by patient breathing and the defects of CT scanner, Figure 5. Mean shift filter is used for edge-preserving smoothing. Convolution and rank filters (such as median filter, mean filter, etc.) could reduced the image noise, but they do not preserve the details and will blur the edges as well.

Mean Shift is a powerful and versatile non parametric iterative algorithm that can be used for lot of purposes like finding modes, clustering, edges etc. Mean Shift was introduced in Fukunaga and Hostetler and has been extended to be applicable in other fields of

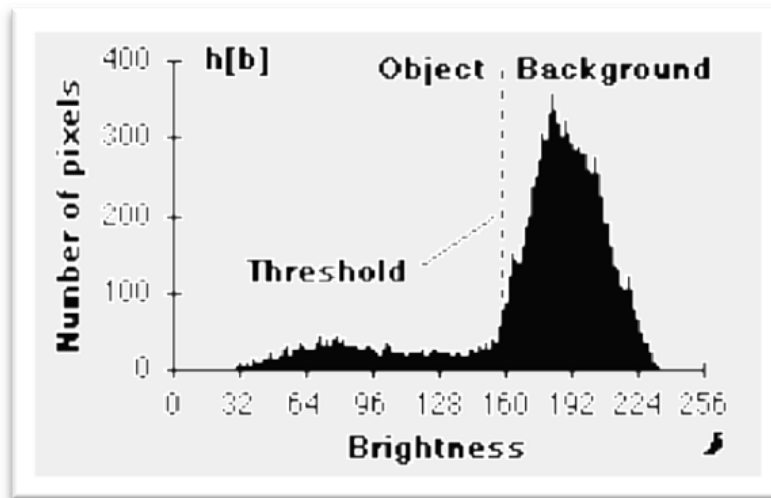


Fig. 3. An example of brightness histogram

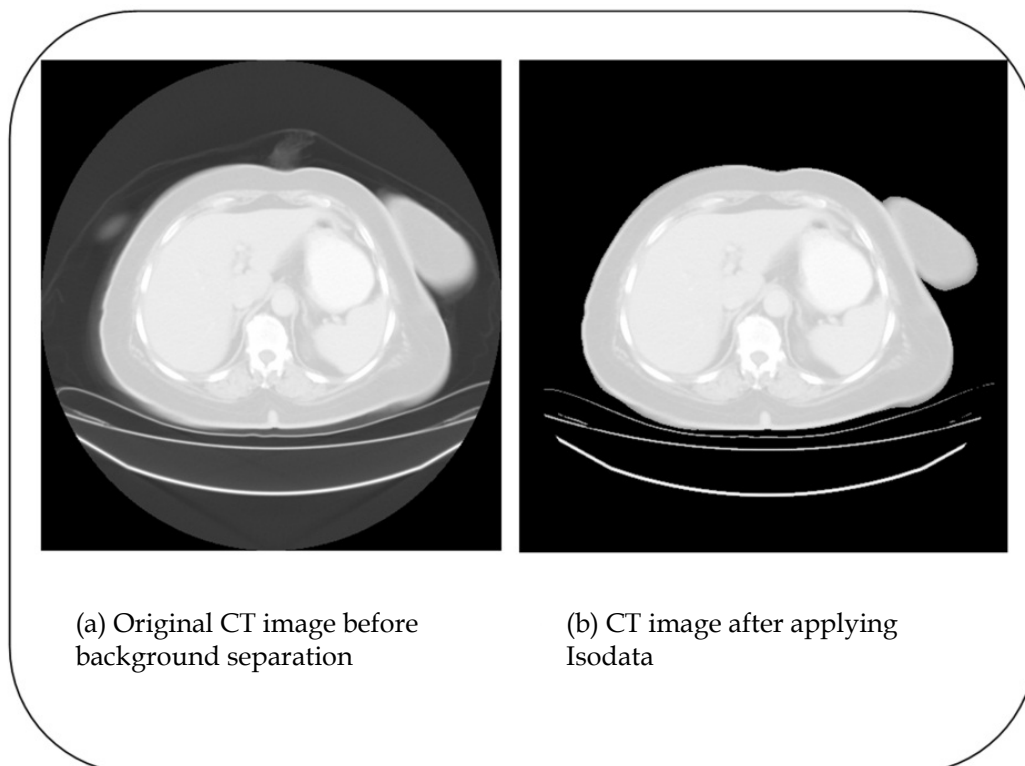


Fig. 4. Block diagram of the proposed automatic liver tumor detection technique

Computer Vision. Mean shift filtering is a data clustering algorithm commonly used in computer vision and image processing. For each pixel of an image (having a spatial location and a particular color), the set of neighboring pixels (within a spatial radius and a defined color distance) is determined. For this set of neighbor pixels, the new spatial center (spatial mean) and the new color mean value are calculated. These calculated mean values will serve as the new center for the next iteration. The described procedure will be iterated until the mean of both spatial and the color (or grayscale) stops changing. At the end of the iteration, the final mean color will be assigned to the starting position of that iteration.

Given an image map  $I(i, j)$  (matrix of which each element represents its corresponding pixel's grey level intensity), a set of data points can be constructed by simply assigning each pixel's location in the map as the first two coordinates, and setting the third coordinate to be the normalized value of the pixel's intensity: for the  $(i, j)$ <sup>th</sup> pixel of the image, the corresponding data point will be:

$$I(i, j) \rightarrow (i, j, I(i, j) * C) \quad (2)$$

where  $C$  is the normalization constant, chosen to be - [average of width and height of image]/[max intensity]:

$$C = \frac{\text{height} + \text{width}}{2} \times \frac{1}{255} \quad (3)$$

The mean shift iteration can be given explicitly by:

$$y_{k+1} = \frac{1}{n_k} \sum_{X_i \in S_h(y_k)} X_i \quad (4)$$

In the  $(k + 1)$ <sup>th</sup> iteration, we shift the current location by the mean position of all data points contained within the sphere of radius  $h$ , centered at  $y_k$ .

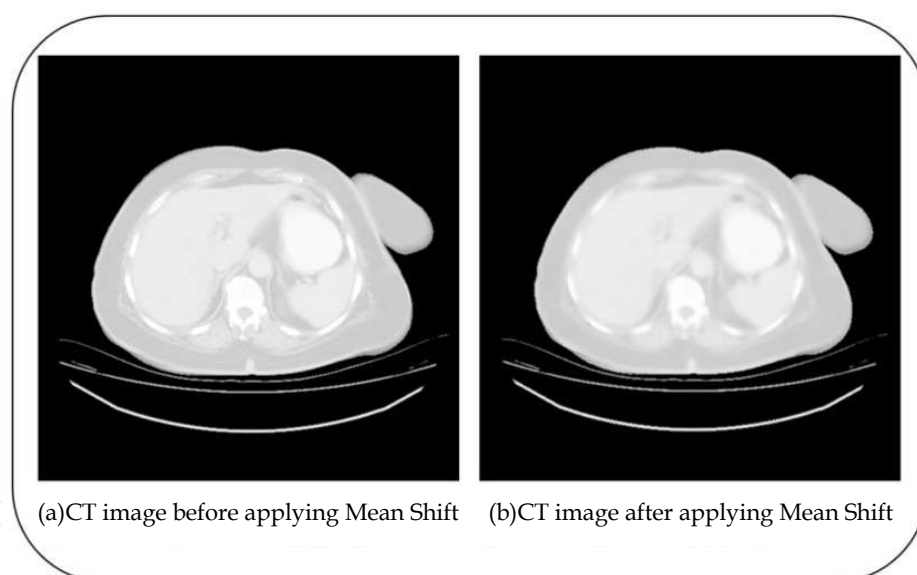


Fig. 5. CT slice before and after Mean Shift smoothing

### 2.1.3 Statistical model

A 3D approach based on statistical information of images and associated to an adaptive threshold technique was implemented in order to recognize the voxels belonging to the liver tissue.

Proper identification of a specific region of interest (ROI) and corresponding definition of the reference key statistics are often crucial points for full automation of algorithms. A technique was developed to find fully automatically this ROI for preventing user dependencies. The proposed algorithm identifies the most liver representative region in the volume dataset as described in the following.

First, each slice of the pre-processed volume is divided into 64 squared regions, as shown in Figure 6., on which the mean image intensity and its standard deviation are calculated (the number and size of these regions had been chosen based on the statistical relevance of estimation samples).

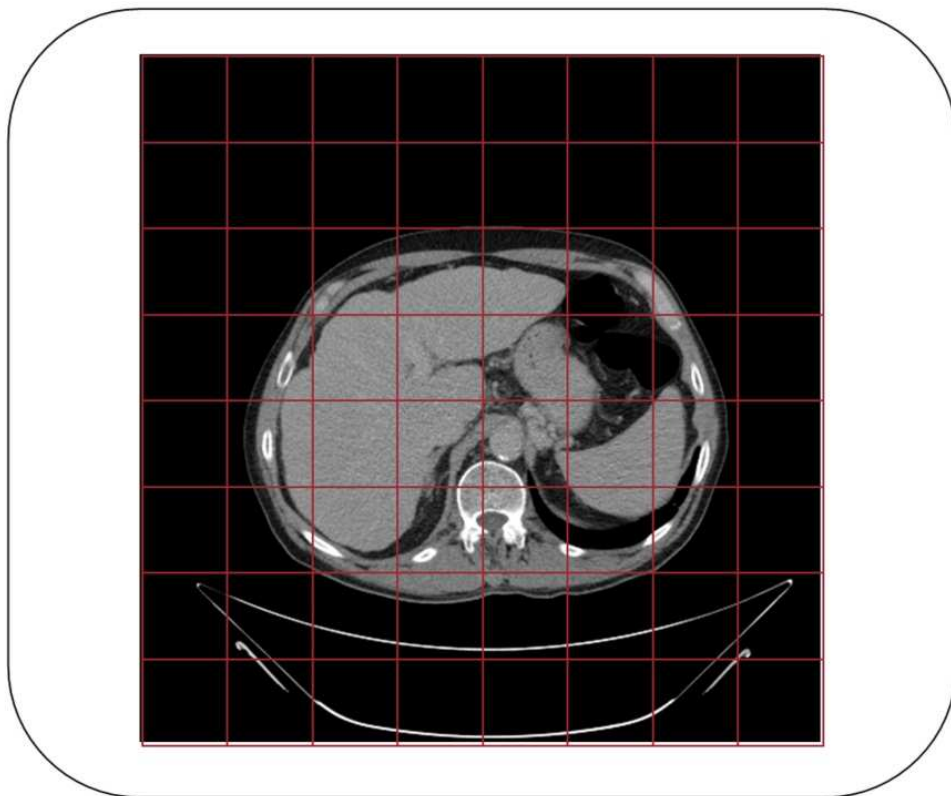


Fig. 6. CT slice is divided into 64 squared regions

Then, the internal abdominal regions having minimal standard deviation (defined as those values lower than 1% of the peak value of corresponding histogram without background) are separated from all volume slices and sorted out in ascending order of mean values. Since the liver is the biggest organ of the abdomen and is homogeneous in terms of image intensity, the great majority of those regions belong to the liver, as shown in Figure 7. Therefore, the  $\mu_{ROI}$  representing the liver tissue is finally selected in this group by choosing the region with the median value of the above-mentioned homogeneous  $\mu_{ROIs}$ . Its statistical information permitted to implement an automatic adaptive histogram-based thresholding technique used to partition images. Therefore, liver voxel recognition depends on patient-specific image datasets since it is calculated automatically through the statistics of the ROI, and not from general learning data analysis. In this work, the threshold was evaluated by using the mean  $\mu_{ROI}$  and the standard deviation  $\sigma_{ROI}$ . Then, a gate function  $G$  is applied to the volume to select the voxels belonging to the liver tissue in function of their image intensity value, defined as follows:

$$G(x, y, z) = \begin{cases} 1 & \text{if } \mu_{ROI} - 2\sigma_{ROI} \leq I(x, y, z) \leq \mu_{ROI} + 2\sigma_{ROI} \\ 0 & \text{else} \end{cases} \quad (5)$$

where  $I(x, y, z)$  is the volume intensity value of the voxel  $(x, y, z)$  in the mean shift-filtered image.

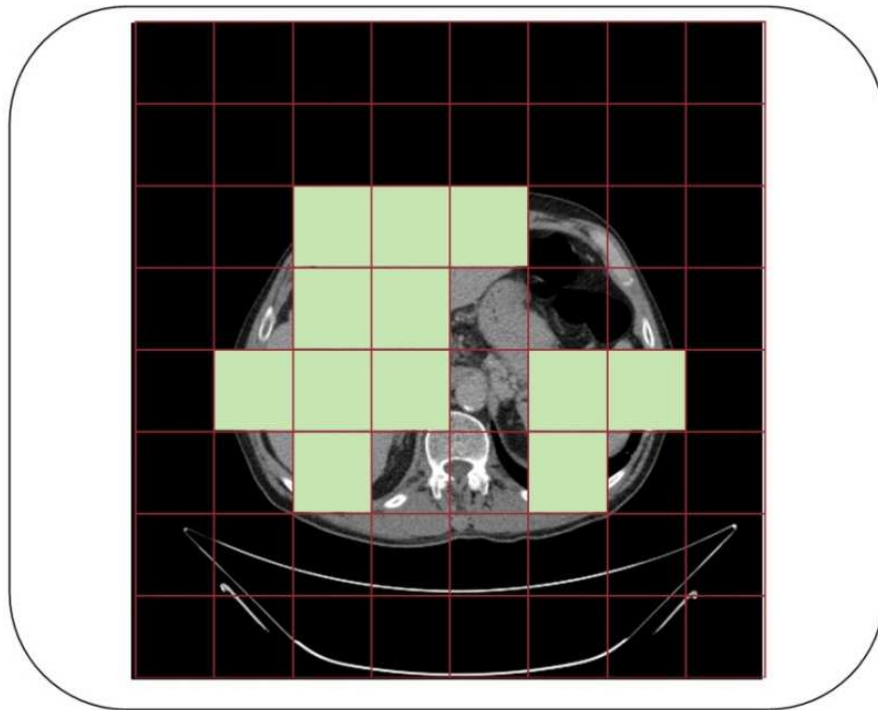


Fig. 7. Determining the squared regions with calculated liver mean ( $\mu_{ROI}$ )

The result of statistical method is a binary image with liver and some parts of organ with similar gray level as black blobs on white background see Figure 8.

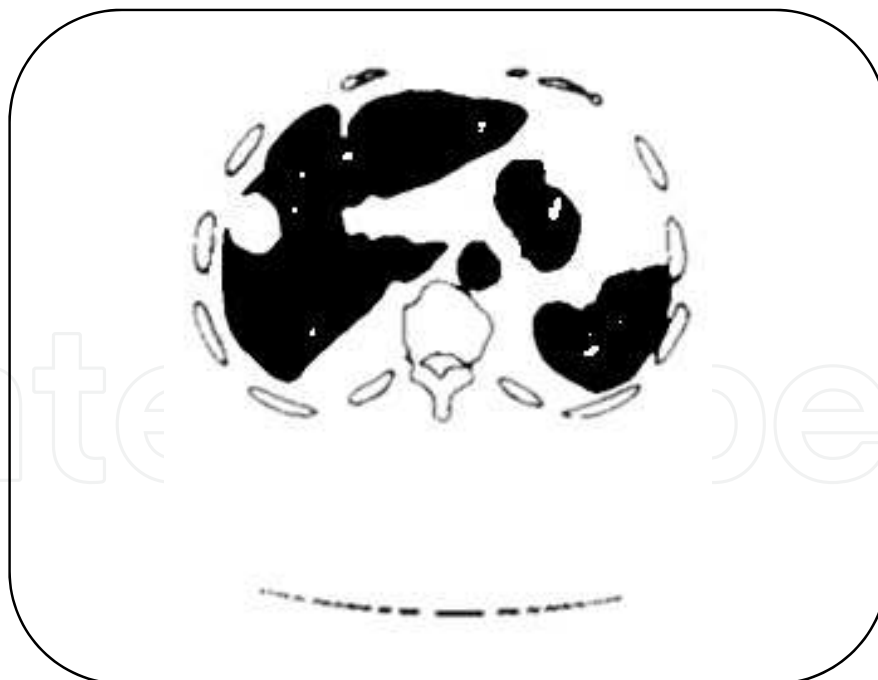


Fig. 8. Thresholding CT slice with the calculated value  $\mu_{ROI}$

#### 2.1.4 Region labeling

In this step, liver is needed to be extracted from other blobs which are the other tissues and organs that share same gray level and turned to be binary. A knowledge-based rule that in

the main slice, where liver is as big as possible, liver structure is the biggest organ in the slice; and so in order to extract the liver region labeling algorithm is used and the biggest label will be that of liver, as shown in Figure 9.

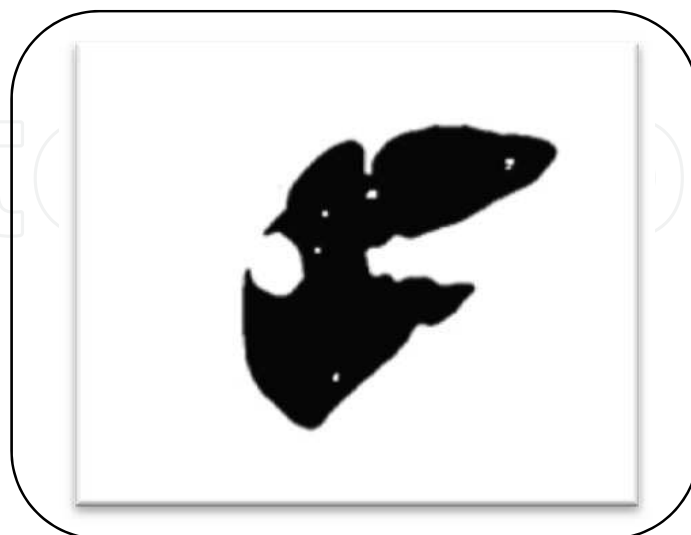


Fig. 9. Labeling the biggest blob

#### 2.1.5 Holes filling

The output of last stage is a black structure with is mostly liver along with some neighboring tissue attached to it because it has close gray level on white background. This black structure contains holes due to existence of vessels, lesion or defects inside liver and when the gate function in statistical model stage is used the irregular pixels of lesion inside liver with will not be considered belonging to liver. The existence of these holes inside liver may hinder the work or snake algorithm that will be used later in following stage to refine final segmentation contour, see Figure 10.



Fig. 10. Hole filling of liver structure



### 2.1.6 Concavity removal

One of the problems that face segmenting liver structure from CT images is the existence of tumor near the edge of liver. In this case, when applying the statistical method to discriminate liver parenchyma from other tissues, tumor tissue will be excluded and hence this will appear like a concave at the edge of segmented liver; That concave may hinder the grow of snake in a following step. A vacancy completely surrounded by liver tissue can be easily filled using simple region filling. However, cancerous tissue is often located adjacent to the border of the liver, as shown in Figure 11.; in this case the area cannot simply be filled as it is open on one side. The proposed method solves this problem using shape information, as the region near the missed area forms a shape like a bay and convex corners remain near the bay.

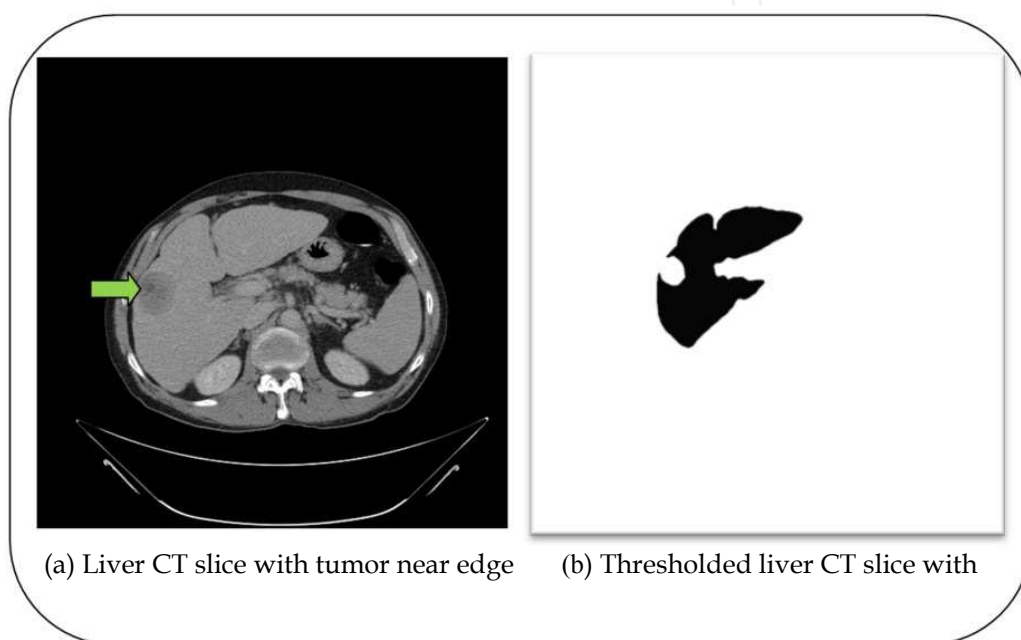


Fig. 11. An example of concave near liver edge due to existence of tumor

Concavity removal consists of three steps; the first step is to identify the outstanding corners around liver structure; the second step is to specify the pair of corners near the missed concave, and the third is filling the missed region to completely recover the liver.

- a. *Identifying the outstanding corners...*The result of hole filling step is first smoothed; then we subtract the smoothed image from the original image (before smoothing) to have image of main corners as a result of subtraction, Figure 12.
- b. *Specifying the pair of corners near the missed concave...*a line between each two pairs of corners is made, and for each line we check for two conditions :
  - i. If the line wholly lies outside live structure.
  - ii. If there is a vacant region inside the line. The vacant region is determined relaying on concavity rate which can be calculated using the formula:

$$\text{Concavity ratio} = \frac{\text{length of perpendicular line between corners line and liver boundary}}{\text{distance between pair of corners}} \quad (6)$$

If the concavity ratio exceeds 125% (empirically predefined value), that vacant is a concave that need to be filled. If there is a line meets these two conditions; that line is probably a line between two corners around concave, shown in Figure 13.



Fig. 12. Identifying the outstanding corners around liver structure

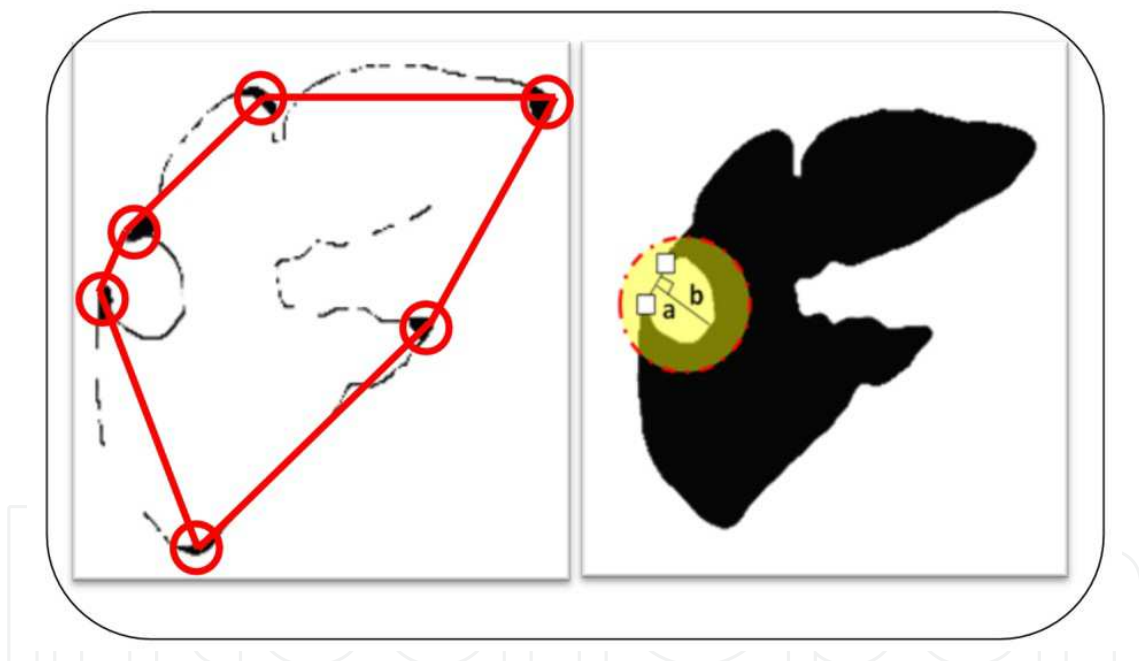


Fig. 13. Specifying the pair of corners near the missed concave

- c. *Filling the missed region...* the pair of points will be linked by an arc (or line) and the region inside an arc is filled the diameter of the arc is determined from the diameter of liver border assuming that the left side of the liver border approximately forms an arc. Using these technique most of missed lesion areas can be successfully corrected.

## 2.2 Refined segmentation

### 2.2.1 Detection the initial contour

After filling the holes inside liver and the concaves near the outer edge of liver, a simple edge detection algorithm is needed to extract the edge of rough segmentation; then the edge



Fig. 14. Filling the concave in liver structure

is treated as a sequence of pixel. The rough segmented contour of liver will be refined in the next stage.

### 2.2.2 The proposed snake algorithm

The concept of active contours models was first introduced in 1987 and has later been developed by different researchers. An active contour is an energy minimizing spline that detects specified features within an image. It is a flexible curve which can be dynamically adapted to required edges or objects in the image.

It consists of a set of control points connected by straight lines, as it is showed in Figure 15. The active contour is defined by the number of control points as well as sequence of each other. Fitting active contours to shapes in images is an interactive process. The user must suggest an initial contour, which is quite close to the intended shape. The contour will then be attracted to features in the image extracted by internal energy creating an attractor image.

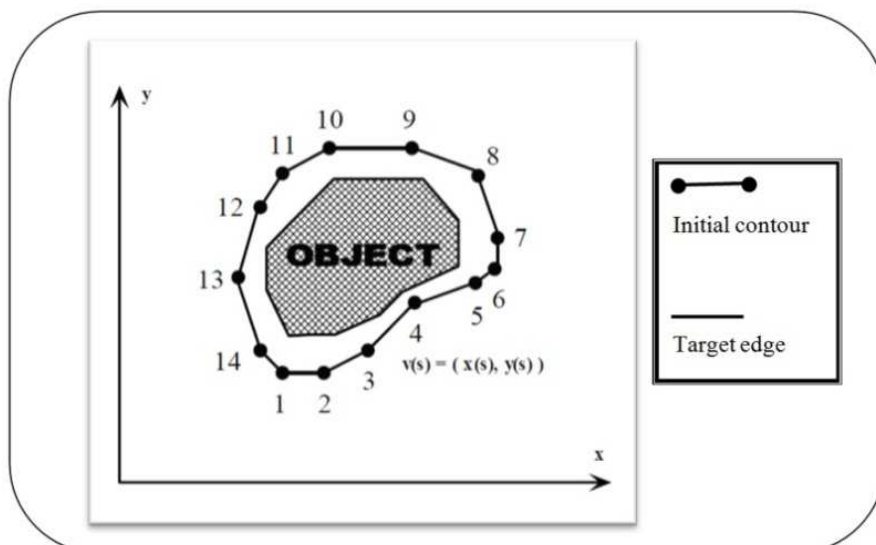


Fig. 15. Snake movement towards final edge

In this study the refinement to the rough segmentation is performed by a new proposed optimized snake technique. The proposed snake algorithm relies mainly on simple computed force not for the entire image, but for specific pixels in a window centered on each pixel of the initial contour; this process is done iteratively and in each iteration the window centered on pixels of initial contour is reduced as the contour approach the final edge of liver. Snake algorithm begins by forming a window and center on each pixel of the initial contour. For each pixel of the final edge which intersects with the window centered on pixels of initial contour, a force is computed using the equation (7):

$$\text{force} = \frac{\text{constant}}{(\text{distance})^2} \quad (7)$$

$$\sin \theta = \frac{\text{opposite}}{\text{distance}} \quad (8)$$

$$\cos \theta = \frac{\text{beside}}{\text{distance}} \quad (9)$$

Then, for each pixel of the true contour of liver in the window we calculate the angles with the pixel of the rough contour centered in the window using the formulas (8) and (9) and as shown in Figure 16.

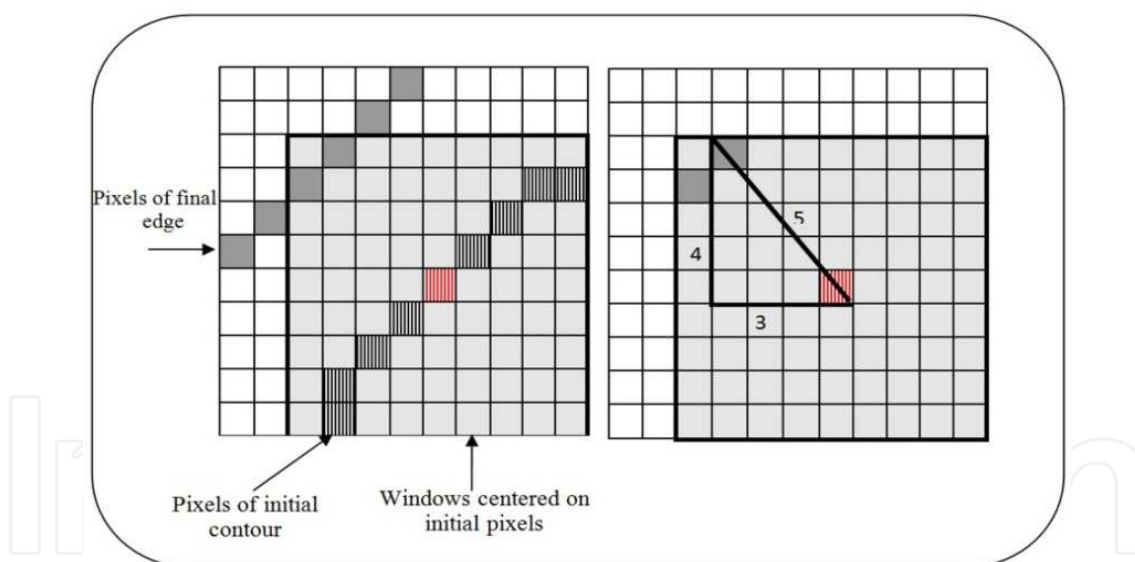


Fig. 16. Calculating force and angle for each pixel of true contour of liver

We use the force and the angle in order to calculate force at X and Y direction ( $X_f$ ,  $Y_f$ ) using formulas (10) and (11):

$$X_f = \text{force} \times \cos \theta \quad (10)$$

$$Y_f = \text{force} \times \sin \theta \quad (11)$$

Then we calculate main force and main angle for all pixels in true contour using formulas (12) and (13):

$$\text{main force} = \sqrt{\sum X_f + \sum Y_f} \quad (12)$$

$$\text{main angel} = \arctan(Y_f / X_f) \quad (13)$$

Using the calculated main force and the main angel, the pixel of initial contour will move to a new location approaching the final edge. The window move to the next pixel and the main force and main angel is calculated again for each pixel of the final edge which intersects with the window centered on the next pixel. After the window finish moving on all the pixels of the initial contour causing the pixels to move a step towards the final edge, the window will iterate over all the pixels of initial contour till it stops moving.

### 3. Liver tumor segmentation

#### 3.1 Tumor detection

##### 3.1.1 Contrast stretching

Having segmented the liver structure in the CT image, the next step is to enhancing the contrast of the segmented slices as liver parenchyma and tumor tissue have similar gray levels. For selecting the stretching range, there is a trade-off between reducing the noise in the image and avoiding over-enhancement.

Linear contract stretching is used to increase the difference between liver tissue and tumors. Among several methods of contract stretching, such as Selective histogram equalization, direct stretching with the linear relationship, linear stretching according to the fitting curve and nonlinear stretching with the logarithmic transformation, direct stretching with the linear relationship shows good result, which can be performed with formula (14):

$$I' = \frac{I'_{\max} - I'_{\min}}{I_{\max} - I_{\min}} (I - I_{\min}) + I'_{\min} \quad (14)$$

where,  $I$  and  $I'$  are the gray levels before and after transformation, respectively.  $I'_{\max}$  and  $I'_{\min}$  are the highest and lowest gray level after transformation,  $I_{\max}$  and  $I_{\min}$  are the maximum and minimum gray level in the liver region before the transformation, respectively.

##### 3.1.2 Add slice to itself

After finishing with contrast enhancement stage, the difference in gray level between liver and tumor is now clear. The gray levels of liver parenchyma are higher than that of tumor tissue as shown in Figure 17. (b). The following step is to add the enhanced image to itself.

$$R(i, j) = I'(i, j) + I'(i, j) \quad (15)$$

After contrast enhancement the pixels of liver parenchyma is brighter, in range between 140 and 160, so that when the value of each pixel is added to itself the value of addition will reach 255 and will appear as white. On the other hand, the pixels which represent tumor tissue is dark with gray level in range between 15 to 40, and so when the value of each tumor pixel is added to itself according to formula (15), the result gray level will be between 30 to 80 appearing as dark spots as shown in Figure 18.

##### 3.1.3 Gaussian blurring

The result of addition is image background as well liver tissue that appears as white background with some pepper noise, and tumors that appear as dark spots with range of

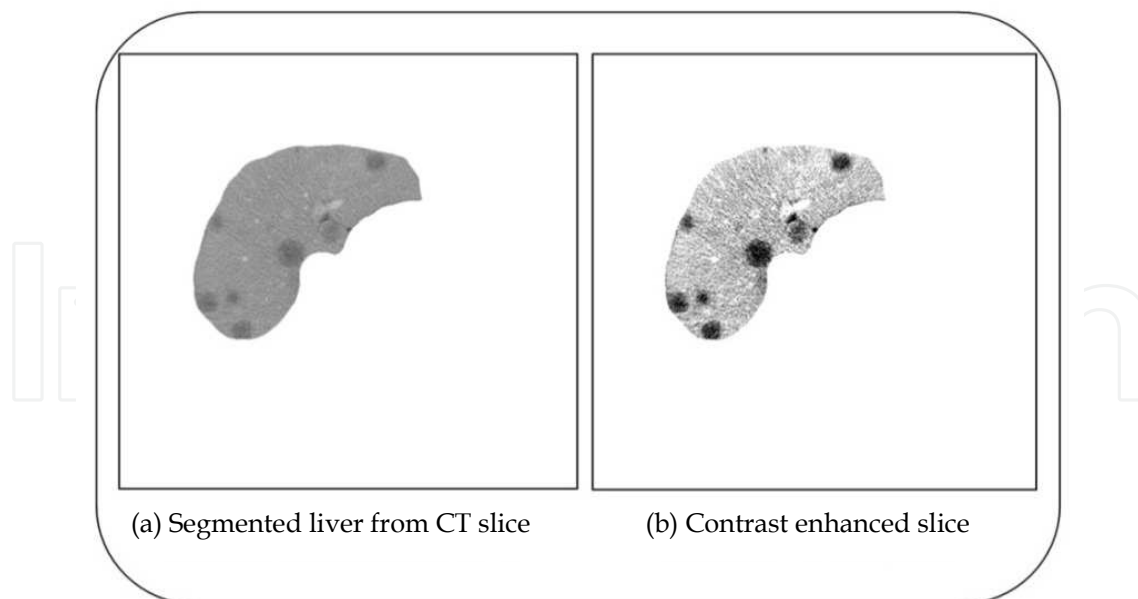


Fig. 17. CT slice before and after contrast enhancement

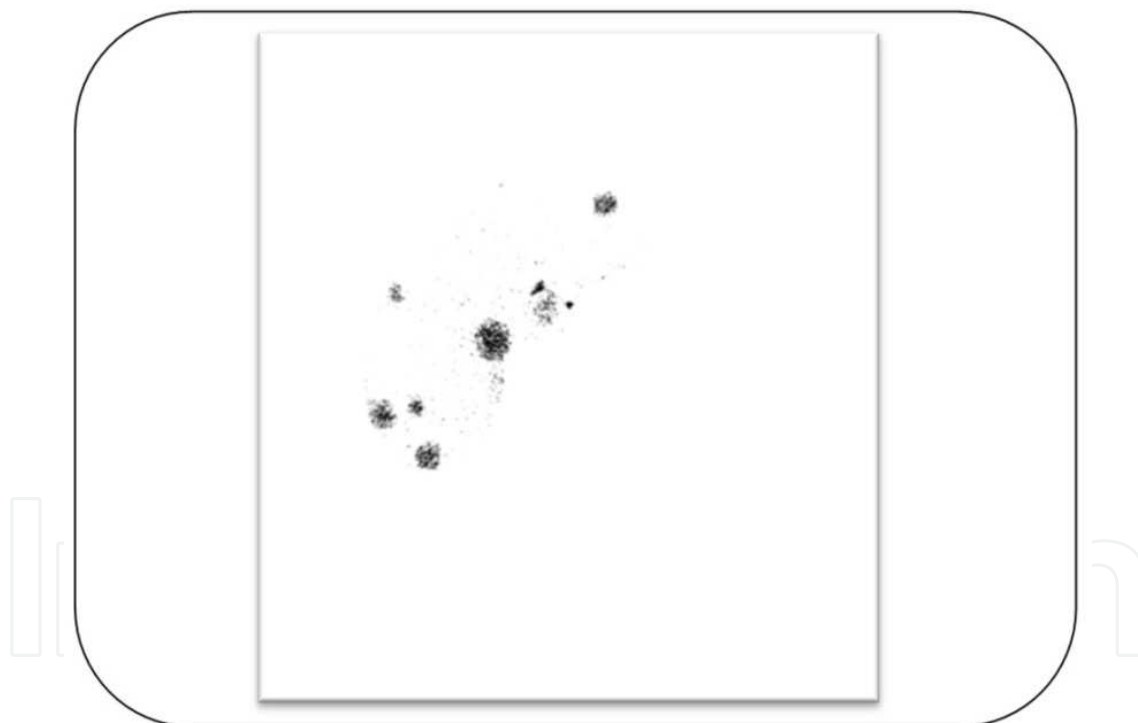


Fig. 18. Result of adding contrast enhanced image to itself

gray levels. In order to remove the noise and make the region of tumor more homogeneous as shown in Figure 19. (a), Gaussian smoothing is used as in formula (16), where  $x$  is the distance from the origin in the horizontal axis,  $y$  is the distance from the origin in the vertical axis, and  $\sigma$  is the standard deviation of the Gaussian distribution.

$$G(x, y) = \frac{1}{\sqrt{2\pi\sigma^2}} e^{-\frac{x^2+y^2}{2\sigma^2}} \quad (16)$$

### 3.1.4 Isodata threshold

As mentioned before, Isodata is a thresholding method which does not need a given threshold value instead the method automatically determine the optimal threshold value. The image after applying Gaussian blurring is a white background with gray blobs which represent liver tumor. When Isodata thresholding technique is applied, the gray blobs will be transformed to be black on white background as shown in Figure 19. (b).

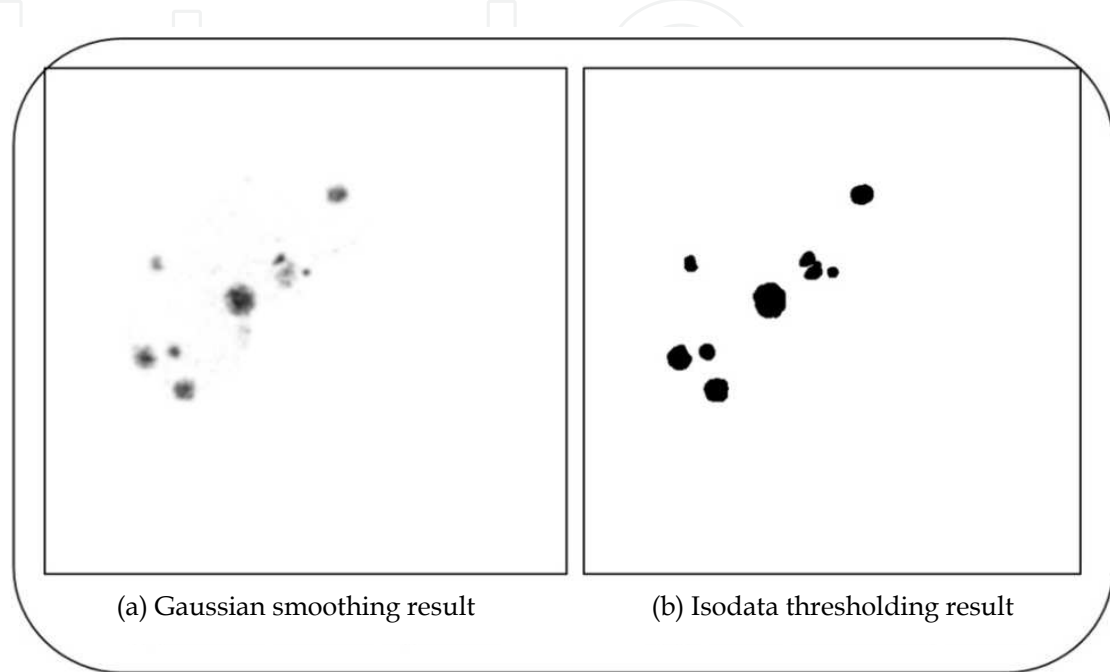


Fig. 19. CT slice before and after Isodata threshold

### 3.1.5 Morphological filters

When Isodata technique is applied the gray blob representing liver tumor along with some scattered noise gray pixels will be turned to black color. In order to remove the noise like pepper pixel, morphological erosion then dilation are used sequentially.

## 3.2 Tumor classification

### 3.2.1 Discriminative rule

The final stage is to eliminate the erroneous segmented tumors. In order to differentiate between a true segmented tumor and CT image defects, a discriminative rule is applied based on medical knowledge that lesion forms a circle-like mass. The circularity of the segmented mass can be defined as in formula number (17):

$$\text{Circularity} = \frac{\text{area of intersection between blob and circle}}{\text{area of formed circle}} \quad (17)$$

The area of the segmented blob is calculated, and then a circle with the same area of the blob is formed. We want to center the circle inside the blob so that all or majority of the circle will be inside the segmented blob. Although there are some algorithms used to detect the center of a blob, yet the irregular shape of blobs may cause misleading result. A simple but effective technique is used; we centered the circle on each pixel of the blob and calculate the intersection between the circle and the blob, we scan with the circle till we get the largest

intersection area; hence the center of the blob is obtained. If the circularity is more than 85%, the segmented blob will be considered as circle-like shape and so it is probably a tumor, as shown in Figure 20.

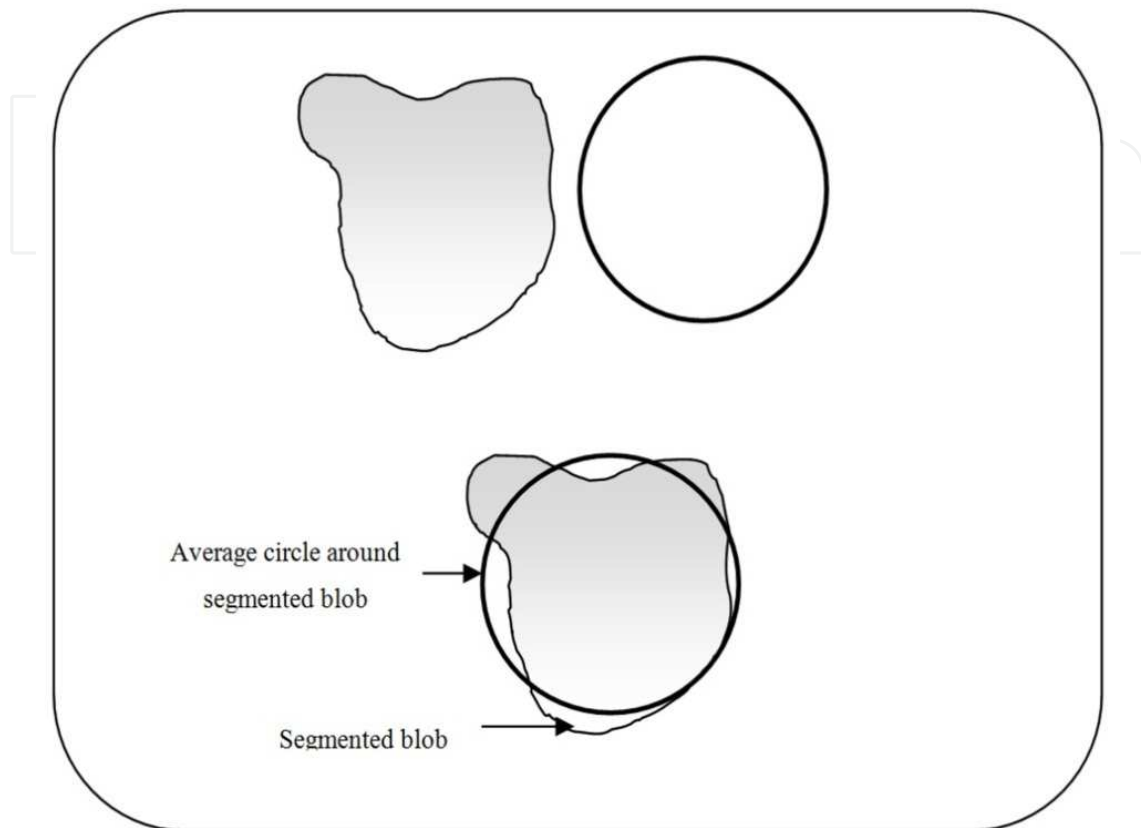


Fig. 20. Knowledge-based circularity rule

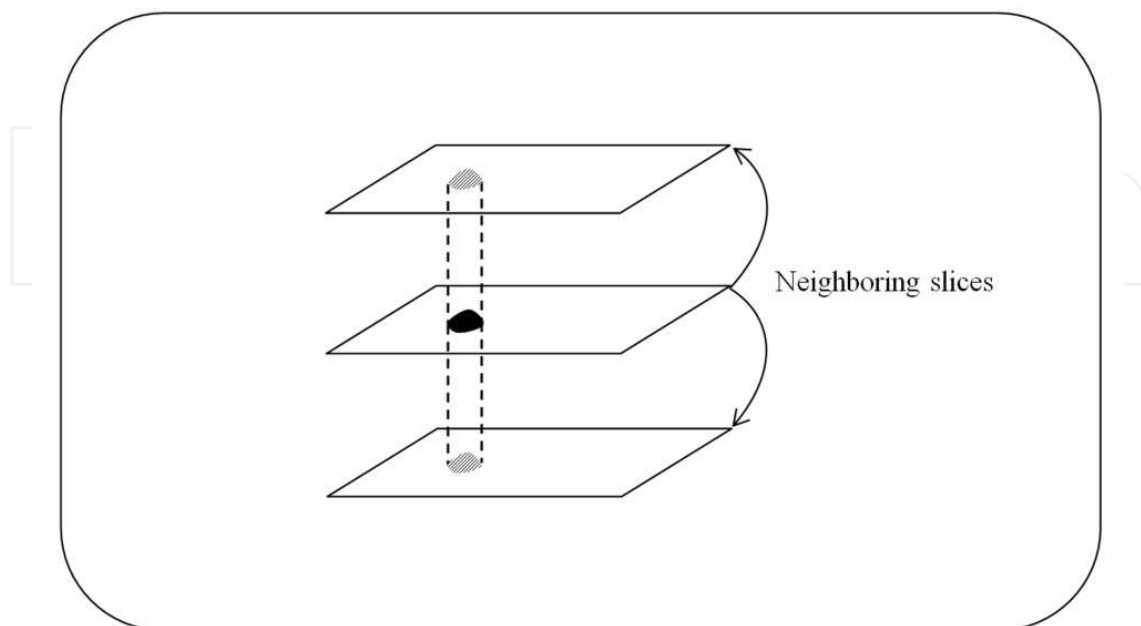


Fig. 21. 3D consistency check with neighboring slices

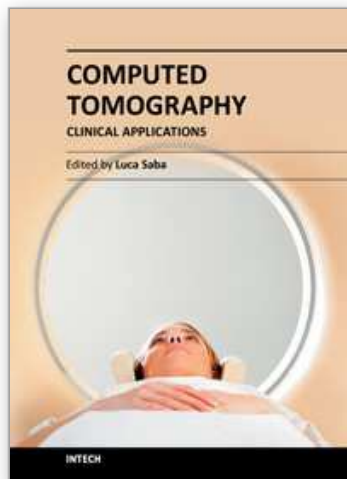


### 3.2.2 3-D consistency check

Another discriminative rule relies on 3-D consistency check is performed based on three-dimensional information that a lesion mass cannot appear in a single slice independently. If a slice has a suspicious tumor and this slice has no interaction with other suspicious tumors in the neighboring slices, this slice with a suspicious tumor will be considered erroneous and the selected blob will be disregarded, Figure 21.

## 4. References

- J.-S. Hong, T. Kaneko, R. Sekiguchi, and K. H. Park, "Automatic Liver Tumor Detection from CT," in *Automatic Liver Tumor Detection from CT- IEICE- TRANSACTIONS on Information and Systems*, 2001, pp. 741-748.
- Y. Liang, *et al.*, "Image enhancement for liver CT images," Shanghai, China, 2009, pp. 75130K-8.
- L. Massoptier, and S. Casciaro, "Fully automatic liver segmentation through graph-cut technique," *Conf Proc IEEE Eng Med Biol Soc*, vol. 2007, pp. 5243-6, 2007.
- L. Massoptier, and S. Casciaro, "A new fully automatic and robust algorithm for fast segmentation of liver tissue and tumors from CT scans," *Eur Radiol*, vol. 18, no. 8, pp. 1658-65, Aug, 2008.
- K. Fukunaga, and L. Hostetler, "The estimation of the gradient of density function, with applications in pattern recognition". *IEEE transactions on Information Theory*, 21(1), 1975, 32-40.
- F. Liu, B. Zhao, P. K. Kijewski, L. Wang, L. H. Schwartz, "Liver segmentation for CT images using GVF snake," *Med Phys*, vol. 32, no. 12, pp. 3699-706, Dec, 2005.
- P. Rodrigues, J. L. Vilaca, and J. Fonseca. "An image processing application for liver tumour segmentation". in *Bioengineering (ENBENG)*, 2011. ENBENG 2011. 1st Portuguese Meeting in. 2011.
- X. Jian-Wu, and K. Suzuki. Computer-aided detection of hepatocellular carcinoma in hepatic CT: False positive reduction with feature selection. 2011 *IEEE International Symposium on Biomedical Imaging: From Nano to Macro*, 2011.
- M. Rudzki, "Automatic image contrast enhancement method for liver vasculature detection". 2011 *Proceedings of the 18th International Conference in Mixed Design of Integrated Circuits and Systems (MIXDES)*, 2011.
- A. H. Foruzan, R. A. Zoroofi, M. Hori, and Y. Sato, "A knowledge-based technique for liver segmentation in CT data," *Comput Med Imaging Graph.*, Vol. 33, pp. 567-587, Dec. 2009.
- Jie L, Lin S, Min D, Yu SCH, Pheng Ann H: "An interactive approach to liver segmentation in CT based on deformable model integrated with attractor force," 2011 *International Conference on Machine Learning and Cybernetics (ICMLC)*, 2011: 1660-1665.
- Haiming A, Chunlan Y, Shuicai W, Yi Z, Song B: "Automatic Segmentation and 3D Reconstruction of Human Liver Based on CT Image," 2010 *4th International Conference on Bioinformatics and Biomedical Engineering (iCBBE)*, 2010: 1-4.



## **Computed Tomography - Clinical Applications**

Edited by Dr. Luca Saba

ISBN 978-953-307-378-1

Hard cover, 342 pages

**Publisher** InTech

**Published online** 05, January, 2012

**Published in print edition** January, 2012

Computed Tomography (CT), and in particular multi-detector-row computed tomography (MDCT), is a powerful non-invasive imaging tool with a number of advantages over the others non-invasive imaging techniques. CT has evolved into an indispensable imaging method in clinical routine. It was the first method to non-invasively acquire images of the inside of the human body that were not biased by superimposition of distinct anatomical structures. The first generation of CT scanners developed in the 1970s and numerous innovations have improved the utility and application field of the CT, such as the introduction of helical systems that allowed the development of the "volumetric CT" concept. In this book we want to explore the applications of CT from medical imaging to other fields like physics, archeology and computer aided diagnosis. Recently interesting technical, anthropomorphic, forensic and archeological as well as paleontological applications of computed tomography have been developed. These applications further strengthen the method as a generic diagnostic tool for non-destructive material testing and three-dimensional visualization beyond its medical use.

### **How to reference**

In order to correctly reference this scholarly work, feel free to copy and paste the following:

Nader H. Abdel-massieh (2012). Fully Automatic Technique for Liver Segmentation from Abdominal CT Scan with Knowledge-Based Constraints, *Computed Tomography - Clinical Applications*, Dr. Luca Saba (Ed.), ISBN: 978-953-307-378-1, InTech, Available from: <http://www.intechopen.com/books/computed-tomography-clinical-applications/fully-automatic-technique-for-liver-segmentation-from-abdominal-ct-scan-with-knowledge-based-constra>

**INTECH**  
open science | open minds

#### **InTech Europe**

University Campus STeP Ri  
Slavka Krautzeka 83/A  
51000 Rijeka, Croatia  
Phone: +385 (51) 770 447  
Fax: +385 (51) 686 166  
[www.intechopen.com](http://www.intechopen.com)

#### **InTech China**

Unit 405, Office Block, Hotel Equatorial Shanghai  
No.65, Yan An Road (West), Shanghai, 200040, China  
中国上海市延安西路65号上海国际贵都大饭店办公楼405单元  
Phone: +86-21-62489820  
Fax: +86-21-62489821

© 2012 The Author(s). Licensee IntechOpen. This is an open access article distributed under the terms of the [Creative Commons Attribution 3.0 License](#), which permits unrestricted use, distribution, and reproduction in any medium, provided the original work is properly cited.

IntechOpen

IntechOpen